where $\beta \approx 3/2$ (see Appendix A).

The parameter b, indicating the decrease of event number with increasing magnitude, was at first considered approximately constant in the Earth (Allen *et al.*, 1965). More specific studies showed that its value could vary both in space (Myamura, 1962) and in time (Healy *et al.*, 1968). Several hypothesis were advanced on the causative physics underlying such distribution, in particular regarding the value of b. It was proposed that b is controlled by fault heterogeneity (Mogi, 1962). A series of experiments on rock samples showed that b could also vary as a function of the imposed stress level (Scholz, 1968). It can be shown that both interpretations are correct and complementary (Wiss, 1973). Assuming that the strength σ_y is a stationary distribution within a rock and that a mean stress $\bar{\sigma}$ can be defined, a relationship can be outlined between b and the probability $F(\sigma_y, \bar{\sigma})$ that the local stress exceeds strength. For example it was proposed (Scholz, 1968) that $b = \nu\ [1 - F(\sigma_y, \bar{\sigma})]$, where ν is a constant and F is an unspecified distribution function. In this paper, we describe a way of altering the distribution $F(\sigma_y, \bar{\sigma})$ by modifying fluid pressure at a rough fault interface, with the consequent change in b.

We postulate that the heterogeneity in fault strength originates in the topographical roughness of the frictional surfaces in contact. Such a model was been proposed as a fault analogy by several authors, who either observed fault roughness in the field (Schmittbuhl *et al.*, 1993) or investigated its consequences on friction (Okubo and Dieterich, 1984; Dieterich, 1994). Normal stress fluctuations caused by roughness reflect onto the fault strength distribution; as we argue further, under such circumstances the fluctuation of fluid pressure may alter the friction and induce time variations in the strength distribution on the fault.

Recent studies have rekindled interest in time variations of b, in particular its possible link to stress level variations prior to critical failure in a rock sample (Sammonds *et al.*, 1992), or prior to the advent of a major earthquake rupture in the Earth crust (Smith, 1981). Time variation of b and its possible mechanical causes are the essential focus of our present study. In particular, we explore its mechanical relation with variations of fluid pressure inside rock pores and fissures. An example of seismicity change linked to pore pressure variations was documented near Denver, Colorado, when injections of high pressure fluid in the ground triggered a relatively abundant seismic activity (Evans, 1966). It was possible to demonstrate the direct influence of pressure on the number of earthquakes but also, to a certain extent, its correlation with the b value in the frequency-magnitude distribution (Healy *et al.*, 1968). It has been argued (Wyss, 1973) that the b change due to pore pressure variations is of the same nature as the b change observed when different stress levels were applied to rock samples in laboratory experiments. Indeed, one consequence of high pore pressure is a drop

in rock strength, which is equivalent to a rise in stress if all other parameters remain unchanged. However, we show hereafter that a pore pressure variation may have more complex and subtle effects on fracture than a change in stress.

In this study we explore in detail the mechanics of faults in the presence of variable pore pressure. We show how the fault properties should be altered in order to obtain a variation of the earthquake distribution, and, in particular, of the b value. The model invokes the presence of fluid-filled, weak zones on the fault that evolve with pore pressure, acting as stress-concentrating flaws inside a fragile system. This creates a bimodal strength distribution, capable of generating fracture distributions with variable b values under variable pressure. In order to test whether the proposed mechanism yields the expected behavior in response to a pressure variation, we simulate fracture on a discrete lattice with spatially inhomogeneous properties under various pressure levels. Such a system shows indeed that the ratio of large to small earthquakes increases when the fluids are drained from the system. This model is attractive because it is builds on a minimum number of basic, well-established assumptions about rocks and fracture mechanics.

We also discuss the relevance of the model with regard to the recent evolution seismicity observed at Mt. Vesuvius, Southern Italy (Zollo *et al.*, 2002).

2. Robustness of the b exponent

We look for a simple mechanism that may induce a significant mutation in the frequency-magnitude distribution of fracture events within a region. We assume that the region, highly permeated with fluids, is undergoing a pore pressure lapse.

The most basic model that we consider involves a fixed fault population (individual faults neither appear nor disappear) with fixed fault sizes. Assume that a drop in pore pressure increases friction by some average amount γ on each fault. Invoking self-similarity, we can assume that γ does not depend on fault size. In such case, the average stress drop $\Delta\bar{\sigma}$ on faults of linear size L will increase to $\gamma\,\Delta\bar{\sigma}$. A fault typically generating an event of moment M_o, will hence release a new moment M_o', that we obtain by integration of the average stress drop over the fault area:

$$M_o = L^3\,\Delta\bar{\sigma} \rightarrow M_o' = \gamma\,L^3\,\Delta\bar{\sigma}\ , \qquad (2)$$

following the definition in Appendix A (note that we dropped a dimensionless geometrical factor of the order of 1 in the expression of the moment, for sake of simplicity).

THE INTERNAL STRUCTURE OF MT. VESUVIUS
Eds. P. Capuano, P. Gasparini, A. Zollo, J. Virieux,
R. Casale and M. Yeroyanni

Pore pressure, earthquake distribution and the cooling of a volcano

Stefan B. Nielsen[1] Aldo Zollo[2] and Warner Marzocchi[1]

[1] *Istituto Nazionale di Geofisica e Vulcanologia, Italy*
[2] *Dip. Scienze Fisiche, Università di Napoli Federico II*

Abstract – Seismic faults may be described as rough failure surfaces pressed together in frictional contact. Most normal load is supported by the protruding asperities, while anti-asperities form areas of loose contact with low frictional strength; such low strength areas act as seeds for nucleation of fracture. As pore pressure increases, the seeds grow in size and number, allowing fracture to be triggered at much weaker tectonic loads; however, fracture has less probability of involving large areas, owing to the low average stress level. This mechanism is illustrated by a rather simple fracture simulation, where it is seen that smaller events are favored at high pore pressure, in such way that the b-value of the magnitude-frequency distribution increases. As an example, we cite the seismicity of Mt. Vesuvius, where a recent drop in temperature and pressure was accompanied by a significant decrease in the seismicity b-value.

keywords: Earthquake distribution, fault mechanics, self-affine surface, cellular automaton model, pore pressure, volcanic seismology

1. Introduction

The number of earthquakes N of magnitude M or greater follow the well-known empirical Gutenberg-Richter frequency-magnitude distribution, stating that in a given sample of events, $\log N = a - b\,M$. This distribution has been abundantly commented in the literature since it was first postulated (Gutenbergand Richter, 1949). The above distribution is equivalent to a power-law expressing the N in terms of the moment M_o:

$$N\,(M_o) \propto M_o^{-b/\beta}\,, \qquad (1)$$

However, since the factor of moment increase is constant throughout the magnitudes, the exponent b in the power law describing the cumulative frequency-moment distribution remains unchanged:

$$N(M_o') = A\,(M_o'/\gamma)^{-b} = A'\,(M_o')^{-b}\,, \tag{3}$$

The same observations applies if we assume that each fault, initially limited to dimension L, extends to cover a dimension L' on average γ times larger that the original one, invoking some effect of increased stress drop on the probability that fracture propagates further (Scholz, 1968). Again, if we assume that γ does not depend on fault dimension because of self-similarity, we can show that b does not change:

$$N(M_o') = A\,(M_o'/\gamma^3)^{-b} = A'\,(M_o')^{-b}\,. \tag{4}$$

Thus the assumption of fixed fault population is not compatible with changes of b, even when allowing self-similar size shift among the fault population.

These examples show that the power-law exponent of the distribution is extremely robust; this feature is well-known in the field of critical phenomena, where the exponents of self-organized systems are only affected by dramatic changes in the internal dynamics. Even different processes can share the same exponents; they are then said to belong to the same universality class (Stanley, 1971).

A more promising mechanism may take place if we assume that the fault population is not fixed (i.e., faults are allowed to appear or disappear), or, alternatively, if we drop the assumption of a self-similar size shift. This imply that the strength distribution should change in a more fundamental way than a simple rescaling. For example, weak patches corresponding to several small, active fault areas may coalesce into larger, stronger faults. Such a mutation may take place when the geometry of a highly heterogeneous system of interacting fractures evolves under the influence of fluids. Another possible consequence of high fluid pressure, over a fault with strong stress fluctuations, is to reduce friction to zero in some patches, thus creating "flaws" in the form of fluid filled pockets. Intuitively, the increasing size and the number of such flaws with pressure will tend to increase the number of small-size fractures that are triggered at the borders of these flaws. There is no simple analytical solution to such problem, but one classical tool for investigation of such a system is the simulation of a discrete system of many interacting elements (Gabrielov et al., 1994).

3. Faulting of rough surfaces under high pore pressure: model and basic assumptions

Next we discuss a few basic assumptions that are built into our fracture model. Measures of the surface roughness on actual fracture surface, among which surfacing fault scarps, consistently yield a self-affine distribution with a roughness (or Hurst exponent) of about $\zeta = 0.85$; this means that the surface is asymptotically flat at large scale, but quite rough at the small scale. If $h(x, y)$ describes the height of a self-affine surface with Hurst exponent ζ, rescaling of the two coordinates $x \rightarrow \lambda x$ and $y \rightarrow \lambda y$ requires a rescaling of height $h \rightarrow h\,\lambda^{\zeta}$ (Feder, 1988). The normal stress across a fault surface is linked to the topography of the two surfaces pressed together. As shown by (Hansen *et al.*, 2000), when the surface is self-affine with a Hurst exponent ζ, the resulting normal stress will also be self-affine, but with an exponent $\zeta - 1$. This is equivalent to a power spectrum distribution, characterizing the elevation in the surface topography, in $\Pi(k) = k^{-1-2\zeta}$ if k is the wavenumber (Schmittbuhl *et al.*, 1993). Finally, we may assume that the power spectrum of normal stress is in $\Pi(k) = k^{-0.7}$.

Furthermore, we assume that yield stress is proportional to the effective normal stress. This can written in the form of a Coulomb law for yield stress, $\sigma_y = \phi\,[\sigma_n]_{eff}$, where ϕ is a dimensionless coefficient of the order of 0.6. The effective normal stress is defined as $[\sigma_n]_{eff} = \sigma_n - P$, i.e., by subtraction of fluid pressure P. At all sites where $P > \sigma_n$, fluid pressure forces the fault borders to open, so that friction is permanently zero and we consider such an area as an open, fluid-filled crack; this assumption is frequently used as a criterion for estimating stress in boreholes by forcing fracture with pressurized mud injection, as described in (Rummel, 1987). At the remaining lattice sites, failure occurs whenever the stress reaches the yield value σ_y defined above. Henceforth we shall use the terms strength, yield stress or σ_y interchangeably.

We have both transient failure, propagating to the solid lattice sites and permanent, fluid filled areas, that act as nucleating points for fracture. Stress is redistributed according to the following conservation rule. For fixed loading conditions at infinity, the net stress flux across our fault surface is a constant (we solve a static problem, so that the system is always at equilibrium). Net stress changes only take place when loading conditions are altered (e.g., stress is slowly increased between fracture events thus simulating the effect of tectonic loading). Thus the shear stress that is not supported inside fluid filled cracks or fractured areas, is redistributed in the unbroken regions. Classical solutions for cracks embedded in an elastic continuum suggest that stress is not redistributed evenly, but is typically concentrated close to the crack, dropping very rapidly away from its border (as $r^{-1/2}$ if r is the distance from the crack tip). Thus we may simplify the

computation by redistributing the stress from a collapsed area only on the first row of cells around the border –typically, a redistribution of load at the crack tip such as that found in Burridge-Knopoff discrete lattice models (Burridge and Knopoff, 1967), or in cellular automata simulating earthquakes as proposed by (Bak and Tang, 1989); however, the interaction rules described below are specific to our model (Fig. 1). We adopt a simplified scalar analogy of the elastic continuum, assuming that there is a single significant stress term σ on the fault. We limit the computation to 2D (the fault surface itself). If at some time t a crack forms, or grows, due to the collapse of N adjacent cells, the integral of stress drop results in a net force

$$\sum_{n=1,N} \sigma(n,t)\,dx^2 \tag{5}$$

where dx^2 is the area of an individual cell and n the cell index. Assuming that such force is redistributed evenly among N_b cells bordering the crack, each of them undergoes a stress increase

$$\Delta\sigma = (1/N_b) \sum_{n=1,N} \sigma(n,t)\,dx^2 \tag{6}$$

As long as new elements fail at the borders of the crack, the fracture event continues and stress is redistributed (Fig. 1 shows an example of fracture on the

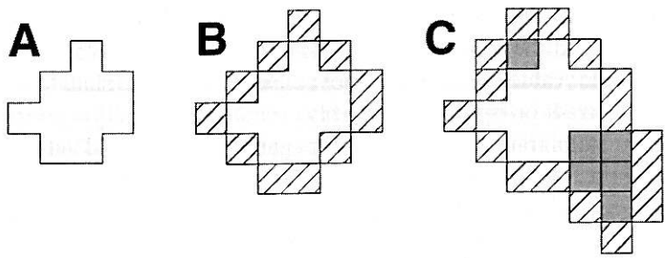

Figure 1. Example of fracture process on the discrete lattice model. (**A**) Permanently fractured, fluid filled area. (**B**) After the system is loaded, the hatched area represents those bordering elements upon which stress from inside the fluid filled crack is evenly redistributed. (**C**) Elements that have reached failure after loading are represented in dark grey. After each element fails, the load is redistributed and it is checked whether more elements have reached the yield limit. After no more elements fail, the moment is computed by summing the stress released from all the failed elements. The hatched area represents the elements where all the load from fracture is finally redistributed. Eventually, all failed elements heal except for the fluid filled crack and stage (**A**) is resumed.

discrete lattice). When failure stops propagating, all sites heal and recover their solid friction, except the fluid filled patches. The moment of the fracture event is computed as the sum of stress drop across the failed area, times an arbitrary elastic stiffness (Appendix A). The system is then loaded again by adding stress until new fractures are initiated. This cycle is iterated several hundred times and we are left

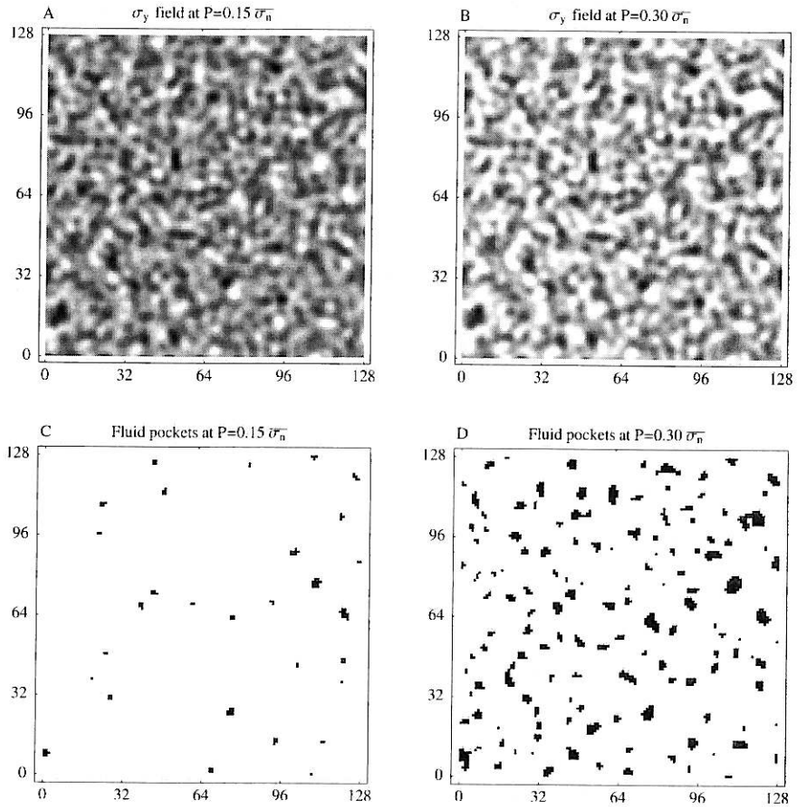

Figure 2. Distribution of yield stress and resulting fluid pockets for two different pressure levels. First, a random field with a power-law spectrum was generated, representing the normal stress distribution on the fault. Then a constant fluid pressure P was subtracted from the field, in order to obtain the effective normal stress and strength σ_y, through a Coulomb friction law (see text for details). The resulting field is represented for (**A**) $P = 0.15\ \bar{\sigma}_n$ and (**B**) $P = 0.30\ \bar{\sigma}_n$, where $\bar{\sigma}_n$ indicates the median value of the normal stress field (the gray scale goes from zero values in white to peak values in black). Finally, those patches where the P exceeds normal stress were defined as open, fluid filled pockets identified by the black spots in (**C**) and (**D**) for low and high pressure levels, respectively. This is only one example among several faults generated with random strength distributions.

with a small stack of moment magnitudes. The whole process can then be repeated for new random distributions of strength; finally, events from all simulations can be merged into a single catalog.

Various random strength distributions with a spectrum in k^{-1} were generated on discrete lattices of 128 × 128 elements, with cutoffs at large and small wavenumbers ($0.05 < k < 0.2$) in order to avoid roughness on a scale smaller that about 5 lattice sites and to account for bridge closure under normal load above a critical crack size (Scholz, 1988). Fracture was simulated for two different levels of pressure, i.e., $P = 0.15\,\bar{\sigma}_n$ and $P = 0.3\,\bar{\sigma}_n$ where the bar indicates the median value (see example of distributions in Fig. 2). By varying the fluid pressure level, we affect the size and the number of the fluid filled areas, and we also affect the overall effective stress distribution (Fig. 3). In order to achieve a statistical significance in the results, the simulations were repeated on lattices with new random distributions, until a satisfactory density of events and convergence of the cumulated results was observed. The cumulative distribution obtained (number of events versus moment) shows a significant decrease in slope associated with the drop in fluid pressure (Fig. 4), in agreement with field observations (Evans, 1966).

The responsible mechanism can be qualitatively explained as follows. At high pore pressure, the fluid pockets are ubiquitous, large and the frictional strength is generally low. Many fracture events are initiated at the edges of the fluid pockets where stress is concentrated, even when the overall load on the system is low. However those fractures often fail to propagate to large areas, because the stress is generally low away from the localized concentrations. On the contrary, when the pressure drops fluid pockets shrink or disappear and the frictional strength rises.

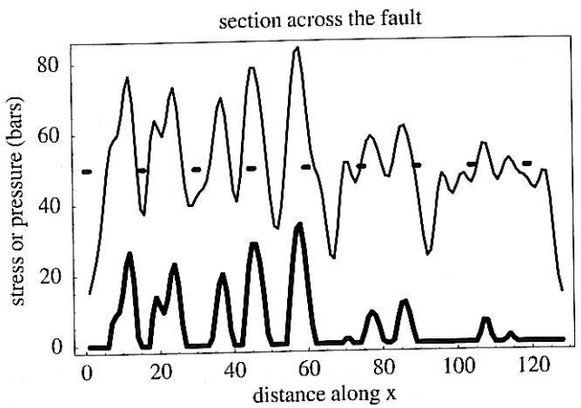

Figure 3. Normal stress (thin curve), pore pressure (dashed line) and resulting strength σ_y (bold curve). This represents a section of Fig. 2 across the fault.

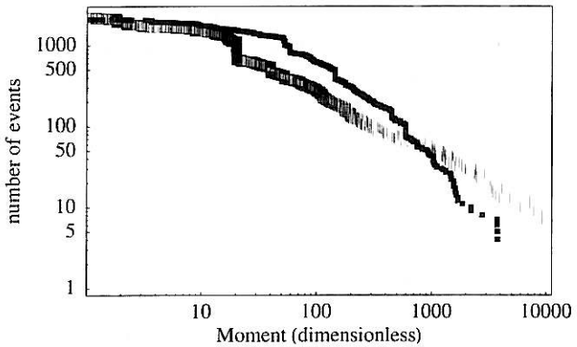

Figure 4. Cumulative distribution of moments obtained by simulating fracture on a set of faults with random strength distributions. Small, solid squares represent events on faults with high pressure ($P = 0.30\,\bar{\sigma}_n$), while large open squares those on faults with low pressure ($P = 0.15\,\bar{\sigma}_n$). Moment is defined as the integral of stress drop across the area failed in a single event. Tapering of the curves at low moment is due to the presence of a smallest scale cutoff, i.e., the size of an elementary cell of the discrete lattice. Note that in the medium-high moment range, the curves both follow a log-linear trend, but the slope is significantly different. Since both distributions were generated on the same fault sets, the only difference is in the pore pressure which alters the strength distribution.

Under such conditions, the load necessary to trigger failure is larger. Once fracture starts, it generally encounters regions under high stress which promote rupture propagation to large areas.

4. Interpreting the recent seismicity of Mt. Vesuvius, Italy

In the case of Mt. Vesuvius, it has been reported (Zollo *et al.*, 2000) that the seismicity over the past three decades was the object of a significant increase of the ratio between large and small earthquakes. Almost in parallel, the temperature measured at the fumerolles has decreased of about 500°C since the last active eruption has terminated in 1944 (Chiodini *et al.*, in press.). Our working hypothesis is that the cooling of the hydraulic system permeating the region, has induced a substantial drop or increase in fluid pressure, thus affecting the friction and the seismicity of the area.

Hence there are two independent observations that we try to relate to the evolution of seismicity, namely, the end of the last active eruptive phase in 1944 and a substantial drop in the temperature measured at the fumerolles at the top of Mt. Vesuvius since the fifties (Chiodini *et al.*, in press.).

It has been pointed out that the value of b – typically fluctuating about 1.3 ± 0.5 – seems to be determined by the particular geological condition of the region (e.g., the tectonic or volcanic activity, the imminence of an eruptive phase, a particular 2 regime or the presence of fluids permeating the crust). In synthesis to the geological and laboratory experiments, it can be argued that the observed b value is low under conditions of low temperatures, relatively high loads, and in non-volcanic, seismically active regions. On the other hand, it is typically high under low loads, high temperatures and in active volcanic regions (Mogi, 1962).

The hydraulics of Mount Vesuvius are obviously characterized by an open system with strong convection and renewal of the fluid mass (other fluids than the magma itself), necessary for the rapid cooling observed, as shown by the ubiquitous presence of fumerolles, ground-water filtration and typical geological markers of volcanic gas expulsion like sulphur crystals.

The functional relation of pressure and temperature in such system is not trivial, since neither the fluid mass nor the confining volume are fixed. However it is a plausible conjecture that a dramatic drop in temperature, inducing the condensation of any vapor phase in the hydrostatic conditions of the topmost Earth's kilometers, should be accompanied by a substantial drop in pressure. Note that in the observed transition from about 600°C to 80°C, the system drops below the triple point in the phase diagram of water.

While we interpret the observed evolution at Mt. Vesuvius in terms of our model of inhomogeneous fault under variable pore pressure, some alternative interpretations have been discussed elsewhere (Zollo *et al.*, 2000). Among others, it was proposed that the seismicity change could be induced by recent magma intrusion, but the authors discarded the hypothesis as inconsistent with the total absence of the typical activity associated tovolcanic events, on one hand, and with the observation of temperature drop, on the other.

5. Acknowledgments

We acknowledge Leon Knopoff and Lucilla de Archangelis for several inspiring discussions. S.N. acknowledges Enzo Boschi, Paolo Gasparini and INGV for support during this study.

References

Aki, K., Scaling law of seismic spectrum, *J. Geophys. Res.*, **72**, 1217-1231, 1967.

Allen, C. R., P. StAmand, C. F. Richter, and J. M. Nordquist, Relationship between seismicity and geologic structure in the Southern California region, *Bull. Seismol. Soc. Am.*, **55**, 753, 1965.

Burridge, R. and L. Knopoff, Model and theoretical seismicity, *Bull. Seismol. Soc. Am.*, **57**, 341-371, 1967.

Bak, P. and C. Tang, Earthquakes as self-organized critical phenomenon, *J. Geophys. Res.*, **94**(B11), 15,635-15,637, 1989.

Chiodini, G., L. Marini, and M. Russo, Geochemical evidence for the existence of high-temperature hydrothermal brines at vesuvio volcano (italy), *Geochim. Cosmochim. Acta*, 2001, In press.

Dieterich, J. H., A constitutive law for rate of earthquake production and its application to earthquake clustering, *J. Geophys. Res.*, **99**, 2601-2618, 1994.

Evans, M. D., Man made earthquakes in denver, *Geotimes*, **10**, 11-18, 1966.

Feder, J., *Fractals*, Plenum Press, 1988.

Gabrielov, A., W. I. Newman, and L. Knopoff, Lattice models of failure: Sensitivity to the local dynamics, *Phys. Rev. E*, **50**(1), 188-197, 1994.

Gutenberg, B. and C. F. Richter, *Seismicity of the Earth*, Princeton Univ. Press, 1949.

Healy, J. H., W. W. Rubey, D. T. Griggs, and C. B. Raleigh, The Denver earthquakes, *Science*, **161**, 1301-1310, 1968.

Hansen, A., J. Schmittbuhl, G. G. Batrouni, and F. A. De Oliveira, Normal stress distribution of rough surfaces in contact, *Geophys. Res. Lett.*, **27**(22), 3639-3642, 2000.

Miyamura, S., The magnitude-frequency relation of earthquakes and its bearing on geotectonics, *Proc. Japan Acad.*, **38**, 27, 1962.

Mogi, K., Magnitude frequency relation for elastic shocks accompanying fracture of various materials and some related problems in earthquakes, *Bull. Earthquake Res. Inst.*, **40**, 831-853, 1962.

Okubo, P. G. and J. Dieterich, Effects of physical fault properties on frictional instabilities produced on simulated faults, *J. Geophys. Res.*, **89**, 5817-5827, 1984.

Rummel, F., Fracture mechanics approach to hydraulic fracturing stress measurements, In Atkinson, B., editor, *Fracture Mechanics of Rock*, pages 217-240. Academic Press, London, 1987.

Scholz, C., The frequency-magnitude relation of microfracturing in rock and its relation to earthquakes, *Bull. Seismol. Soc. Am.*, **58**(1), 399-415, 1968.

Scholz, C. H., The critical slip distance for seismic faulting, *Nature*, *336*, 761-763, 1988.

Schmittbuhl, J., S. Gentier, and S. Roux, Field measurements of the roughness of fault surfaces, *Geophys. Res. Lett.*, **20**, 639-641, 1993.

Smith, W. D., The b-value as an earthquake precursor, *Nature*, *289*, 136-139, 1981.

Sammonds, P. R., P. G. Meredith, and I. G. Main, Role of pore fluids in the generation of seismic precursors to shear fracture, *Nature*, **359**, 228-230, 1992.

Stanley, H. E., *Introduction to Phase Transitions and Critical Phenomena*, Oxford University Press, New York, 1971, International Series of Monographs on Physics.

Wyss, M., Towards a physical understanding of the earthquake frequency distribution, *Geophys. J. R. Astron. Soc.*, **31**, 341-59, 1973.

Zollo, A., W. Marzocchi, P. Capuano, A. Lomax, and G. Iannaccone, Space and time behaviour of seismic activity at mt. vesuvius volcano, southern italy, *Bull. Seismol. Soc. Am.*, **92**, 2, 625-640, 2002.

Appendix A: Moment definition

The seismic moment is a measure of earthquake size; it is defined as the integral of the dislocation that occurred on the fault area during the earthquake, times the shear stiffness μ of the medium:

$$M_o = \mu \iint_{\Gamma} \Delta u(\mathbf{x})\, dx\, dy \tag{7}$$

where Δu is the final dislocation and $\mathbf{x}$ a point of the fault surface Γ. Assuming average values of dislocation $\Delta\bar{u}$ and stress drop $\Delta\bar{\sigma}$, and a linear dimension L of the fault, we have $\Delta\bar{\sigma} = C\mu\,\Delta\bar{u}/L$, where C is a dimensionless geometrical factor of the order of 1 that depends on the fault shape (in our simulation we assume that $C \approx 1$ for all fractures). The above definition of moment expressed in terms of average stress yields:

$$M_o = C\, L^3\, \Delta\bar{\sigma} \tag{8}$$

The magnitude M is another familiar measure of earthquake size; it can be defined in a number of ways, making it a more arbitrary quantity. Following Aki (1967), we shall assume in our discussion that magnitude and moment are related by: $\beta\, M = \log M_o - \alpha$. Combining such relation with the frequency-magnitude law $\log N = a - b\, M$, we obtain the moment distribution (Eq. 1). Note that α and β can be estimated either theoretically or empirically; typical values are of the order of $\alpha \approx 17$ and $\beta \approx 3/2$.